A Simple Dufort-Frankel-type Scheme for the Gross-Pitaevskii Equation of Bose-Einstein Condensates on Different Geometries

Ming-Chih Lai,[1] **Chung-Yin Huang,**[2] **Te-Sheng Lin**[2]
[1]*Department of Applied Mathematics, National Chiao Tung University, 1001, Ta Hsueh Road, Hsinchu 300, Taiwan*

[2]*Department of Mathematics, National Chung Cheng University, Minghsiung, Chiayi 621, Taiwan*

Received 15 July 2003; accepted 15 December 2003
Published online 26 February 2004 in Wiley InterScience (www.interscience.wiley.com).
DOI 10.1002/num.20008

We develop a simple Dufort-Frankel-type scheme for solving the time-dependent Gross-Pitaevskii equation (GPE). The GPE is a nonlinear Schrödinger equation describing the Bose-Einstein condensation (BEC) at very low temperature. Three different geometries including 1D spherically symmetric, 2D cylindrically symmetric, and 3D anisotropic Cartesian domains are considered. The present finite difference method is explicit, linearly unconditional stable and is able to handle the coordinate singularities in a natural way. Furthermore, the scheme is time reversible and satisfies a discrete analogue of density conservation law. © 2004 Wiley Periodicals, Inc. Numer Methods Partial Differential Eq 20: 624–638, 2004

Keywords: Dufort-Frankel scheme; Gross-Pitaevskii equation; nonlinear Schrödinger equation; Bose-Einstein condensates

I. INTRODUCTION

Recently, the Bose-Einstein condensate (BEC) has been observed in dilute atomic vapor of ^{87}Rb atoms by confining magnetic traps at ultra-low temperature [1, 2]. This successful experiment has spurred a great interest in the study of experimental, theoretical [3], numerical investigations on various aspects of the condensate [4–8], and the references therein. The condensate usually consists of a few thousand to millions of atoms confined by the trap potential. This is a complicated many-body problem whose complete description would involve a fully understanding of quantum kinetics. However, at very low temperature, the dynamics of a finite, dilute system of weakly interacting bosons can be well captured by the Gross-Pitaevskii theory [9, 10].

Correspondence to: Ming-Chih Lai, Department of Applied Mathematics, National Chiao Tung University, 1001, Ta Hsueh Road, Hsinchu 30050, Taiwan (e-mail: mclai@math.nctu.edu.tw)
Contract grant sponsor: National Science Council of Taiwan; contract grant number: NSC-92-2115-M-009-012

The Gross-Pitaevskii equation (GPE) [9, 10] of the condensate wave function ψ has the form

$$i\hbar \frac{\partial \psi}{\partial t} = -\frac{\hbar^2}{2m}\Delta\psi + V(\mathbf{x})\psi + U_0|\psi|^2\psi, \tag{1.1}$$

where in quantum mechanics, the quantity $|\psi|^2$ represents the density distribution of the atoms. Thus, the total number of atoms N in the condensate equals to

$$N = \int_{R^3} |\psi(\mathbf{x}, t)|^2 d\mathbf{x}. \tag{1.2}$$

The parameter m is the atomic mass, $\hbar$ is the Planck constant, and the U_0 describes the interaction between atoms with the form

$$U_0 = \frac{4\pi\hbar^2 a}{m}, \tag{1.3}$$

where a is the s-wave scattering length. Note that, $a > 0$ represents for a repulsive interaction, whereas $a < 0$ for attractive interaction. The Equation (1.1) was derived independently by Gross [9] and Pitaevskii [10] in the 1960s. Its validity is based on the assumption that the s-wave scattering length must be much smaller than the average distance between atoms and that the number of atoms in the condensate be much larger than one. Thus, at very low temperature, the GPE can be used to explore the macroscopic behavior of the condensate.

The external trap potential $V(\mathbf{x})$ is usually chosen in the form of a harmonic well,

$$V(\mathbf{x}) = \frac{m}{2}(\omega_x^2 x^2 + \omega_y^2 y^2 + \omega_z^2 z^2), \tag{1.4}$$

where ω_x, ω_y, and ω_z are the angular trap frequencies in the x, y, and z direction.

To make the equation dimensionless, we first introduce the following characteristic length and time units:

$$S_l = \sqrt{\frac{\hbar}{m\omega_x}}, \qquad S_t = \frac{1}{\omega_x}. \tag{1.5}$$

We then scale the space, time, and the wave function by those units; that is,

$$\tilde{\mathbf{x}} = \frac{\mathbf{x}}{S_l}, \qquad \tilde{t} = \frac{t}{S_t}, \qquad \tilde{\psi} = \frac{S_l^{3/2}\psi}{\sqrt{N}}. \tag{1.6}$$

After some careful calculation, we obtain the dimensionless GPE (after dropping the tilde notation) as

$$i\frac{\partial \psi}{\partial t} = -\frac{1}{2}\Delta\psi + V(\mathbf{x})\psi + \kappa|\psi|^2\psi, \tag{1.7}$$

where the harmonic trap potential becomes

$$V(\mathbf{x}) = \frac{1}{2}(x^2 + \gamma_y^2 y^2 + \gamma_z^2 z^2), \qquad \gamma_y = \frac{\omega_y}{\omega_x}, \qquad \gamma_z = \frac{\omega_z}{\omega_x}, \tag{1.8}$$

and the parameter κ is

$$\kappa = \frac{4\pi Na}{S_l}. \tag{1.9}$$

The density conservation law (1.2) now becomes the normalizing condition

$$\int_{R^3} |\psi(\mathbf{x}, t)|^2 d\mathbf{x} = 1. \tag{1.10}$$

One should note that the above conservation of the position density can be easily derived from the Equation (1.7) itself under the assumption of the same normalizing condition for the initial value.

The main goal of this article is to introduce a simple finite difference scheme to solve the dimensionless GPE (1.7) on different symmetric geometries. There are a few numerical approaches in the literature. For instance, in [4], the author used the Crank-Nicolson scheme to study the spherically symmetric GPE in two space dimensions. This is a semi-implicit scheme, meaning that the nonlinear term of $|\psi|^2$ is treated explicitly, whereas the linear term is treated implicitly. This scheme is first-order accurate in time and second-order in space as shown in [5]. The first-order accuracy in time might be attributed to the way of discretization of $|\psi|^2$ term. If we use the Adams-Bashforth method to discretize the $|\psi|^2$ term, then the scheme becomes second-order in time and space. This linearized Crank-Nicolson scheme was developed in [8] for solving the generalized nonlinear Schrödinger equation. However, the Crank-Nicolson type of scheme involves solving a linear system of equations whose diagonal entries change at each time step. Such computational complexity becomes very impractical in the case of three-dimensional BEC simulation.

One alternative to avoid solving linear system of equations is to use an explicit scheme. In [6], the authors used an explicit finite difference method called the synchronous Visscher scheme to simulate the GPE in 2D cylindrical geometry. Notice that, this method is nothing but the well-known leap-frog scheme [11], which is applied to integrate certain time-dependent PDEs. As the authors mentioned, the other contribution of their article is the careful treatment near the axis (coordinate singularity). However, the leap-frog scheme has a very restrictive stability constraint so the time step must be chosen one order smaller than the spatial mesh, which makes the method less efficient for the long-time integration.

Another explicit type scheme called Dufort-Frankel method has been applied to solve the linear and nonlinear one-dimensional Schrödinger equations [12]. The method is very similar to the leap-frog scheme but has better numerical stability (see the comparison in the next section).

The scheme is time reversible just as the Schrödinger equation. Furthermore, the grid analogue of density conservation law (1.10) has been established by different authors [12–14] to study the convergence and stability of the method. In particular, Markowich et al. [14] apply the Wigner-measure analysis to investigate the convergence of the Dufort-Frankel scheme for the Schrödinger equation in a semi-classical regime.

In this article, we shall extend the Dufort-Frankel method to solve the Gross-Pitaevskii equation (1.7) on different symmetric geometries. We will introduce a simple but different spatial discretization from [4, 6, 7, 15] to handle the coordinate singularities occurring in spherical and cylindrical geometries. Besides, we will derive a discrete analogue of density conservation law for the scheme on the spherically symmetric case. To the best of our knowledge, this is the first time such a scheme has been applied to the context of BEC problems.

Recently, Bao et al. have proposed an elegant time-splitting spectral method (TSSP) to solve the linear [16] and nonlinear [17] Schrödinger equations in the semi-classical regime. Their method is based on time splitting (two steps) the nonlinear Schrödinger equation in a clever way so that the solution can be integrated exactly in each time step. The method is second-order accurate in time and spectral accurate in space. Furthermore, the scheme is explicit, unconditionally stable, time reversible, and time transverse invariant and conserves the position density at discrete level. Comparing to the Dufort-Frankel scheme, the TSSP method only needs an additional Fast Fourier Transform (FFT) employed at each time step so the method is very efficient. The approach has also been applied to solve the GPE in Cartesian coordinates [5] and in the radial and cylindrical coordinates [18]. Note that, it is not our intention to compare or compete with the TSSP method. Instead, here we just try to introduce a simple and explicit finite difference alternative to simulate the time-dependent BEC problem.

The rest of the article is organized as follows. In Section 2, we make a comparison of the leap-frog and the Dufort-Frankel schemes by considering the one-dimensional linear Schrödinger equation. We then write down the detailed time and spatial discretization for the Dufort-Frankel type scheme on different geometries in Section 3. The numerical test results are given in Section 4 and followed by some conclusions. In the Appendix, we derive a discrete conservation law of the position density for the present Dufort-Frankel scheme on 1D spherically symmetric domain.

II. LEAP-FROG VS. DUFORT-FRANKEL SCHEME

In this section, we shall compare the leap-frog and Dufort-Frankel schemes. We will show that although both schemes are explicit, the leap-frog scheme is conditionally stable while the Dufort-Frankel scheme is unconditionally stable. For simplicity, we consider the following one-dimensional linear equation:

$$i\frac{\partial \psi}{\partial t} = -\frac{1}{2}\frac{\partial^2 \psi}{\partial x^2} + V_0\psi. \tag{2.1}$$

The potential here is simply chosen as a positive constant $V(x) = V_0$.

The leap-frog scheme for the Equation (2.1) is

$$i\frac{\psi_j^{n+1} - \psi_j^{n-1}}{2\Delta t} = -\frac{1}{2}\frac{\psi_{j+1}^n - 2\psi_j^n + \psi_{j-1}^n}{\Delta x^2} + V_0\psi_j^n. \tag{2.2}$$

One can easily see that the scheme is explicit and the truncation error is of order $O(\Delta t^2 + \Delta x^2)$. To see the stability, let us apply the von Neumann analysis by writing the discrete solution as

$$\psi_j^n = \lambda^n e^{ik(j\Delta x)}. \tag{2.3}$$

Substituting the expansion into (2.2) and manipulating the algebra a bit, we can get the quadratic equation of the amplification factor as

$$\lambda^2 + 2i(\mu(1 - \cos k\Delta x) + \Delta t V_0)\lambda - 1 = 0, \tag{2.4}$$

where

$$\mu = \frac{\Delta t}{\Delta x^2}. \tag{2.5}$$

Thus, the roots of the above equation are

$$\lambda_\pm = -i(\mu(1 - \cos k\Delta x) + \Delta t V_0) \pm \sqrt{1 - (\mu(1 - \cos k\Delta x) + \Delta t V_0)^2}. \tag{2.6}$$

It can be checked easily that $|\lambda_\pm| = 1$, if the stability constraint

$$2\mu + \Delta t V_0 \le 1, \tag{2.7}$$

is satisfied. So the leap-frog scheme is conditionally stable.

The Dufort-Frankel scheme for the Equation (2.1) is simply to replace the term ψ_j^n by $(\psi_j^{n+1} + \psi_j^{n-1})/2$ in the leap-frog (2.2); that is,

$$i\,\frac{\psi_j^{n+1} - \psi_j^{n-1}}{2\Delta t} = -\frac{1}{2}\,\frac{\psi_{j+1}^n - (\psi_j^{n+1} + \psi_j^{n-1}) + \psi_{j-1}^n}{\Delta x^2} + V_0\,\frac{\psi_j^{n+1} + \psi_j^{n-1}}{2}. \tag{2.8}$$

One can easily check that the truncation error is of order $O(\Delta t^2 + \Delta x^2 + (\Delta t/\Delta x)^2)$. The scheme is again explicit since the right-hand side term involves only ψ_j^{n+1} term (no ψ_{j+1}^{n+1} and ψ_{j-1}^{n+1} terms). Applying the von Neumann analysis, we can get the quadratic equation of the amplification factor as

$$(1 + i(\mu + \Delta t V_0))\lambda^2 - (2i\mu \cos k\Delta x)\lambda - (1 - i(\mu + \Delta t V_0)) = 0. \tag{2.9}$$

The roots of the above equation are

$$\lambda_\pm = \frac{i\mu \cos k\Delta x \pm \sqrt{-\mu^2 \cos^2 k\Delta x + 1 + (\mu + \Delta t V_0)^2}}{1 + i(\mu + \Delta t V_0)}. \tag{2.10}$$

Note that, the term inside the square root is always positive; thus, it can be checked easily that $|\lambda_\pm| = 1$, for any μ. This concludes that the scheme is unconditionally stable. However, in order

to ensure the consistency, the meshes should satisfy $\Delta t/\Delta x \to 0$ as the meshes Δt, Δx go to zero. Therefore, the key to the convergence is the consistency rather than the stability of the scheme.

III. DUFORT-FRANKEL SCHEME FOR GPE ON DIFFERENT GEOMETRIES

In this section, we will present the detailed time and spatial discretization of Dufort-Frankel scheme for the GPE (1.7) in different geometries. Those geometries include the 1D spherically symmetric, 2D cylindrically symmetric, and 3D anisotropic Cartesian domains. One should realize that those geometries we considered here are strongly related to the form of the trap potential via the choice of γ_y and γ_z in (1.8). Notice that, the present Dufort-Frankel scheme is time reversible just like the Equation (1.7) and satisfies a discrete analogue of density conservation law (see the Appendix in detail).

A. 1D Spherically Symmetric Case

For the isotropic case (i.e., $\gamma_y = \gamma_z = 1$), the BEC ground state wave function is spherically symmetric [15]. Thus, the 3D GPE (1.7) with spherical symmetry can be simply reduced to an effective 1D equation as

$$i\frac{\partial \psi}{\partial t} = -\frac{1}{2}\left(\frac{\partial^2 \psi}{\partial r^2} + \frac{2}{r}\frac{\partial \psi}{\partial r}\right) + \frac{1}{2}r^2\psi + \kappa|\psi|^2\psi, \tag{3.1}$$

with the normalizing condition

$$4\pi \int_0^\infty |\psi|^2 r^2 dr = 1. \tag{3.2}$$

The traditional numerical approach [15] is first to write the wave function as a new function divided by $1/r$ term, then substitute this new form into the Equation (3.1) to eliminate the first derivative term. In order to integrate the equation, the behavior at $r = 0$ must be derived. However, one can see that is not necessary in our finite difference discretization as follows.

Because the solution decays very fast in the radial direction, we simply pick a large domain $[0, R]$ such that the solution is set to be $\psi(R, t) = 0$. We then choose a uniform spatial grid $r_j = j\Delta r, j = 1, 2, \ldots, M$ with $\Delta r = R/(M + 1)$ and a temporal grid $t_n = n\Delta t$ with the time step $\Delta t > 0$. Now we discretize the Equation (3.1) by the Dufort-Frankel type scheme:

$$i\frac{\psi_j^{n+1} - \psi_j^{n-1}}{2\Delta t} = -\frac{1}{2}\left(\frac{\psi_{j+1}^n - (\psi_j^{n+1} + \psi_j^{n-1}) + \psi_{j-1}^n}{\Delta r^2} + \frac{2}{r_j}\frac{\psi_{j+1}^n - \psi_{j-1}^n}{2\Delta r}\right) + \frac{1}{2}r_j^2\frac{\psi_j^{n+1} + \psi_j^{n-1}}{2} + \kappa\left|\frac{\psi_j^{n+1} + \psi_j^{n-1}}{2}\right|^2\frac{\psi_j^{n+1} + \psi_j^{n-1}}{2}, \tag{3.3}$$

where the solution ψ_j^n is considered an approximation of $\psi(r_j, t_n)$. Unlike the explicit treatment for the $|\psi|^2$ term used in the work [12, 13], we discretize the nonlinear term implicitly too. So in order to find ψ_j^{n+1}, we need to solve a complex cubic equation of $(\psi_j^{n+1} + \psi_j^{n-1}/2)$. However, this can be done analytically and no extra work is needed. Besides, when the index $j = 1$ of (3.3),

it can be observed that the coefficient of ψ_0^n equals to zero. Thus, there is no need to find the numerical boundary value ψ_0^n so that no pole condition is needed. Therefore, the coordinate singularity can be handled more naturally than in [15].

B. 2D Cylindrically Symmetric Case

In the earlier BEC experiments, the external potential is typically chosen in the form of cylindrical trap ($\gamma_y = 1$, $\gamma_z \neq 1$), so that the number γ_z determines the aspect ratio of the trap. With cylindrical symmetry, the 3D GPE can be simply reduced to an effective 2D equation as

$$i\frac{\partial \psi}{\partial t} = -\frac{1}{2}\left(\frac{\partial^2 \psi}{\partial r^2} + \frac{1}{r}\frac{\partial \psi}{\partial r} + \frac{\partial^2 \psi}{\partial z^2}\right) + \frac{1}{2}(r^2 + \gamma_z^2 z^2)\psi + \kappa|\psi|^2\psi, \tag{3.4}$$

with the normalizing condition

$$2\pi \int_{-\infty}^{\infty}\int_{0}^{\infty} |\psi|^2 r dr dz = 1. \tag{3.5}$$

As in the 1D spherically symmetric case, we simply choose a computational domain $\Omega = [0, R] \times [-L_z/2, L_z/2]$ in $r - z$ plane such that the solution is set to be zero outside this domain. That is, we set $\psi(R, z, t) = 0$ and $\psi(r, -L_z/2, t) = \psi(r, L_z/2, t) = 0$. Again, like the 1D isotropic case, most of existing numerical methods such as the one in [6] need to have specific treatment at the origin. In the next, we will see this is not necessary in our finite difference discretization.

We first choose a shifted grid [19] as

$$(r_j, z_k) = ((j - 1/2)\Delta r, -L_z/2 + k\Delta z), \qquad 1 \le j \le M, 1 \le k \le L, \tag{3.6}$$

where $\Delta r = 2R/(2M + 1)$ and $\Delta z = L_z/(L + 1)$. Now we write down the Dufort-Frankel type scheme for the Equation (3.4) by

$$\begin{aligned} i\frac{\psi_{jk}^{n+1} - \psi_{jk}^{n-1}}{2\Delta t} = -\frac{1}{2}\Bigg(&\frac{\psi_{j+1,k}^n - (\psi_{jk}^{n+1} + \psi_{jk}^{n-1}) + \psi_{j-1,k}^n}{\Delta r^2} + \frac{1}{r_j}\frac{\psi_{j+1,k}^n - \psi_{j-1,k}^n}{2\Delta r} \\ &+ \frac{\psi_{j,k+1}^n - (\psi_{jk}^{n+1} + \psi_{jk}^{n-1}) + \psi_{j,k-1}^n}{\Delta z^2}\Bigg) + \frac{1}{2}(r_j^2 + \gamma_z^2 z_k^2)\frac{\psi_{jk}^{n+1} + \psi_{jk}^{n-1}}{2} \\ &+ \kappa\left|\frac{\psi_{jk}^{n+1} + \psi_{jk}^{n-1}}{2}\right|^2 \frac{\psi_{jk}^{n+1} + \psi_{jk}^{n-1}}{2}. \end{aligned} \tag{3.7}$$

Note that, by choosing such grid, we avoid placing the grid point directly at the origin. When the index $j = 1$ in (3.7), the coefficient of ψ_{0k}^n equals to zero since $r_1 = \Delta r/2$. Once again, we do not have to find the numerical boundary value ψ_{0k}^n so that no pole condition at $r = 0$ is needed. This concludes that our scheme is more succinct than the scheme with pole conditions.

C. 3D Anisotropic Case

Now we consider the 3D anisotropic case without any symmetry ($\gamma_y \neq \gamma_z \neq 1$). The 3D GPE is written in Cartesian coordinates with the form (1.7). As the previous two cases, we choose a

3D computational domain $\Omega = [-L_x/2, L_x/2] \times [-L_y/2, L_y/2] \times [-L_z/2, L_z/2]$, such that the solution is set to be zero outside this domain. We then define a uniform grid in this computational domain by

$$(x_j, y_k, z_l) = (-L_x/2 + j\Delta x, -L_y/2 + k\Delta y, -L_z/2 + l\Delta z). \tag{3.8}$$

The 3D GPE (1.7) can be discretized by the Dufort-Frankel method as

$$\begin{aligned} i\,\frac{\psi_{j,k,l}^{n+1} - \psi_{j,k,l}^{n-1}}{2\Delta t} = &-\frac{1}{2}\left(\frac{\psi_{j+1,k,l}^{n} - (\psi_{j,k,l}^{n+1} + \psi_{j,k,l}^{n-1}) + \psi_{j-1,k,l}^{n}}{\Delta x^2} + \frac{\psi_{j,k+1,l}^{n} - (\psi_{j,k,l}^{n+1} + \psi_{j,k,l}^{n-1}) + \psi_{j,k-1,l}^{n}}{\Delta y^2}\right. \\ &\left. + \frac{\psi_{j,k,l+1}^{n} - (\psi_{j,k,l}^{n+1} + \psi_{j,k,l}^{n-1}) + \psi_{j,k,l-1}^{n}}{\Delta z^2}\right) + \frac{1}{2}\,(x_j^2 + \gamma_y^2 y_k^2 + \gamma_z^2 z_l^2)\,\frac{\psi_{j,k,l}^{n+1} + \psi_{j,k,l}^{n-1}}{2} \\ &+ \kappa\left|\frac{\psi_{j,k,l}^{n+1} + \psi_{j,k,l}^{n-1}}{2}\right|^2 \frac{\psi_{j,k,l}^{n+1} + \psi_{j,k,l}^{n-1}}{2}. \end{aligned} \tag{3.9}$$

Here, the numerical boundary values in x, y, and z directions are all given by the zero boundary conditions.

IV. NUMERICAL RESULTS

In this section, we perform a series of tests for the Dufort-Frankel type scheme developed in the previous section. Those test problems consist of the accuracy check of 1D spherically symmetric case, the free expansion of 2D cylindrically symmetric condensate and the 3D simulation of the anisotropic condensate. To quantify the numerical results, we define the condensate width σ_x along x-axis as

$$\sigma_x = \sqrt{\langle (x - \langle x \rangle)^2 \rangle}, \tag{4.1}$$

where the bracket $\langle \cdot \rangle$ denotes the space averaging with respect to the position density:

$$\langle f \rangle \equiv \int_\Omega f(\mathbf{x}) |\psi(\mathbf{x}, t)|^2 d\mathbf{x}. \tag{4.2}$$

As we can see from the probability theory, the bracket $\langle \cdot \rangle$ represents the expected value while the condensate width σ_x represents the standard deviation. Similarly, we can define the condensate widths σ_y, σ_z, and σ_r of y, z, and r directions in the same manner.

Example 1. The accuracy check of 1D spherically symmetric case: In the first test, we consider the following 1D accuracy check. The idea is to construct an exact solution for the 1D spherically symmetric GPE (3.1) and then apply the 1D Dufort-Frankel scheme (3.3) to obtain the numerical solution. To proceed, we need to find the ground state solution within the formalism of mean-field theory. For this, the condensate wave function can be written as

TABLE I. Three different errors for $\||\psi_e|^2 - |\psi_c|^2\|_\infty$, $\|Re(\psi_e - \psi_c)\|_\infty$, and $\|Im(\psi_e - \psi_c)\|_\infty$ at $T = 5$.

Δr	Δt	$\||\psi_e\|^2 - \|\psi_c\|^2\|_\infty$	Rate	$\|Re(\psi_e - \psi_c)\|_\infty$	Rate	$\|Im(\psi_e - \psi_c)\|_\infty$	Rate
$\frac{1}{10}$	$\frac{1}{100}$	8.7241e-004	—	0.0645	—	0.1024	—
$\frac{1}{20}$	$\frac{1}{400}$	2.6937e-004	1.70	0.0115	2.49	0.0294	1.80
$\frac{1}{40}$	$\frac{1}{1600}$	7.4881e-005	1.85	0.0026	2.15	0.0076	1.95

$$\psi(r, t) = e^{-i\mu t}\phi(r), \tag{4.3}$$

where μ is the chemical potential and ϕ is a time-independent real function. Then the Gross-Pitaevskii equation becomes

$$\mu\phi = -\frac{1}{2}\left(\frac{\partial^2\phi}{\partial r^2} + \frac{2}{r}\frac{\partial\phi}{\partial r}\right) + \frac{1}{2}r^2\phi + \kappa|\phi|^2\phi, \tag{4.4}$$

subject to the same normalizing condition (3.2) for ϕ. Obviously, we have $|\psi(r, t)|^2 = |\psi(r, 0)|^2 = \phi^2(r)$, meaning that the density profile has the same shape as the ground state density.

Instead of solving the nonlinear eigenvalue problem (4.4) directly, we use the same Dufort-Frankel scheme to compute the ground state solution by solving the normalized gradient flow to its steady state [20]. This approach of finding the ground state is called the imaginary-time method, which is popularly used in physics literatures. Once we obtain the μ and $\phi(r)$, we can construct the exact wave function by the Equation (4.3).

Now we apply the 1D scheme (3.3) to integrate the spherically symmetric GPE (3.1). The initial condition $\psi(r, 0)$ is chosen as the computed ground state solution $\phi(r)$. Table I shows the grid refinement results for our Dufort-Frankel scheme. The error is measured by the maximal norm of the difference between the exact solution ψ_e given by (4.3) and the computed solution ψ_c. We compute three different errors: $\||\psi_e|^2 - |\psi_c|^2\|_\infty$, real part $\|Re(\psi_e - \psi_c)\|_\infty$, and imaginary part $\|Im(\psi_e - \psi_c)\|_\infty$ errors. In our test, the parameter $\kappa = 100$.

As mentioned in Section 2, the truncation error of the Dufort-Frankel scheme is $O(\Delta t^2 + \Delta r^2 + (\Delta t/\Delta r)^2)$. One can easily see that if we choose the time step $\Delta t = \Delta r^2$, then we expect second-order convergence as the mesh is refined. This is indeed the case as we see from Table I. However, using these meshes, the leap-frog scheme is unstable.

Figure 1(a) shows the plot of the computed density solution $|\psi|^2$ at $T = 5$ and the ground state solution $\phi^2 = |\psi(r, 0)|^2$. One can see they coincide with each other quite well. Figure 1(b) is the evolutionary plot of the l_2 norm of $|\psi|$. One can see that our scheme actually preserves the normalizing condition (3.2) very well too.

Example 2. Free expansion of 2D cylindrically symmetric condensate: In this example, we consider the free expansion of 2D cylindrical self-interacting condensate [21]. Such a situation is realized in experiments by first evaporative cooling an almost pure condensate in which the noncondensate portion is less than 20%. We then allow the cloud to expand freely by suddenly turning off the confining potential.

In order to simulate this problem, as in [6], we start with an elongated condensate wave function as

$$\psi(r, z, 0) = \frac{\gamma_z^{1/4}}{(12.5\pi)^{3/4}}\exp(-0.04(r^2 + \gamma_z^2 z^2)), \tag{4.5}$$

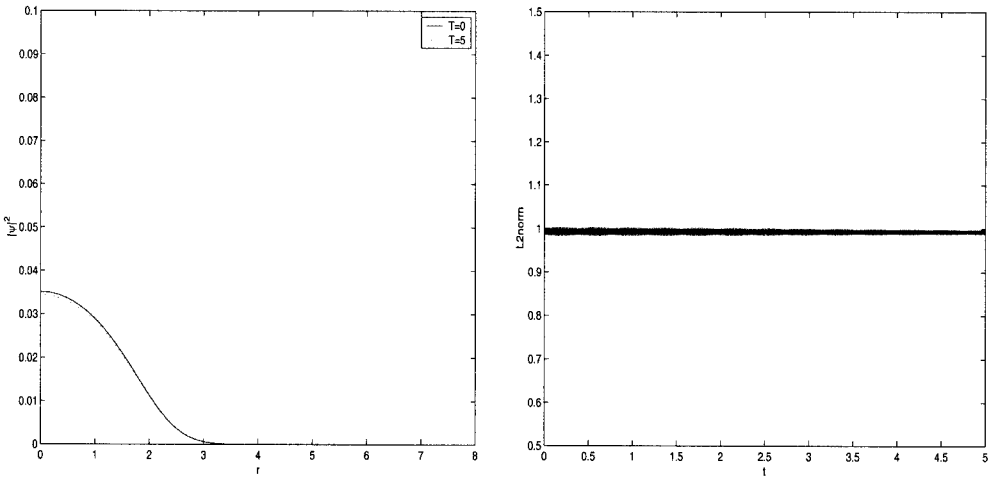

FIG. 1. (a) The plot of computed density $|\psi(r, T = 5)|^2$ and the ground state density $|\phi|^2 = |\psi(r, 0)|^2$. (b) The time evolutionary plot of l_2 norm of $|\psi|$.

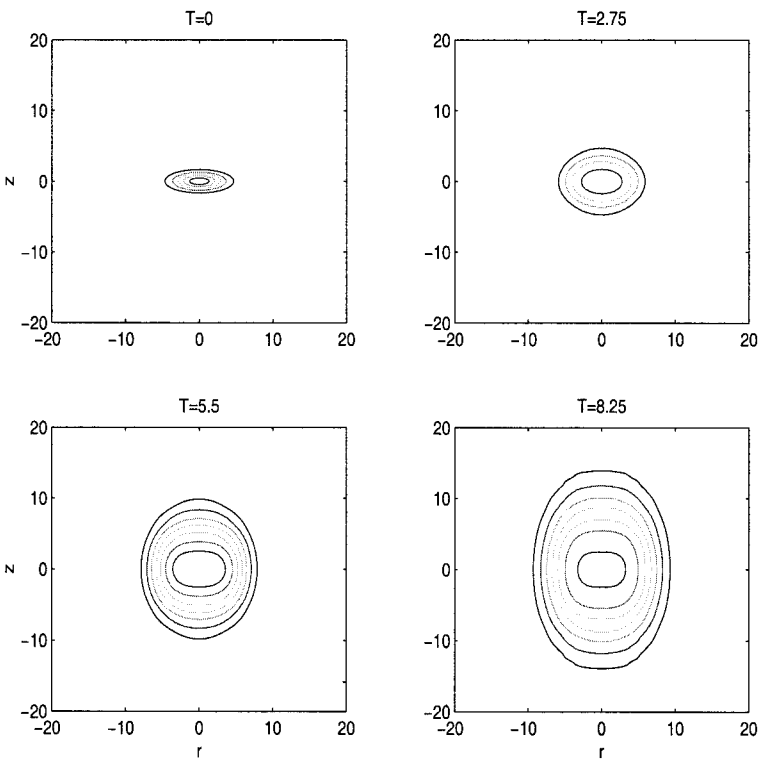

FIG. 2. The snapshots of the density $|\psi|^2$ profile at different times for the free expansion of 2D cylindrical condensate.

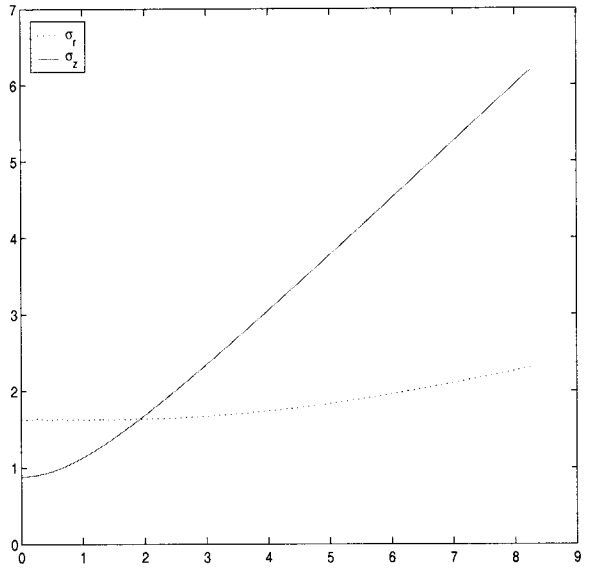

FIG. 3. The time evolutionary plot of the 2D condensate widths σ_r and σ_z.

with the aspect ratio $\gamma_z = \sqrt{8}$ as in [6]. At time $t = 0^+$, we turn off the trap potential to let the condensate expand freely; that is, we use the scheme (3.7) to evolve the 2D GPE (3.4) without the trap potential term. The computational domain is chosen as $[0, 20] \times [-20, 20]$ in the $r - z$ plane. The mesh width is chosen as $\Delta r = \Delta z = 0.1$ and the time step $\Delta t = 0.01$. The parameter $\kappa = 100$ corresponds to thousands of bosons in physical units.

Figure 2 shows four snapshots of contour images of the condensate density function $|\psi|^2$. One can see that the condensate is initially confined more strongly in the axial (z) direction than in the radial (r) direction. Once the trap potential is removed, the condensate proceeds an expansion where the thin portion of condensate expands faster than the thick one. This phenomenon has been confirmed from the contour plots as well as the condensate widths plots in Figure 3.

Example 3. 3D anisotropic defocusing condensate: We now perform the anisotropic test by simulating the 3D defocusing condensate [5]. As in [5], the initial condition is taken as

$$\psi(x, y, z, 0) = \frac{(\gamma_y \gamma_z)^{1/4}}{\pi^{3/4}} \exp(-(x^2 + \gamma_y y^2 + \gamma_z z^2)/2). \tag{4.6}$$

The computational domain is chosen as $\Omega = [-8, 8]^3$. We use the mesh $\Delta x = \Delta y = \Delta z = 1/8$ and the time step $\Delta t = 0.001$.

Figure 4 shows the condensate widths as a function of time for the anisotropic condensate of $\gamma_y = 2$ and $\gamma_z = 4$ for the weakly interacting case $\kappa = 10$. One can see the time frequencies of the condensate widths σ_y and σ_z are roughly two and four times of the frequency of σ_x, respectively. This result coincides with the frequency ratios γ_y and γ_z perfectly, which also shows a good agreement with the one obtained in [5]. Thus, the numerical evidence confirms the validness of our scheme.

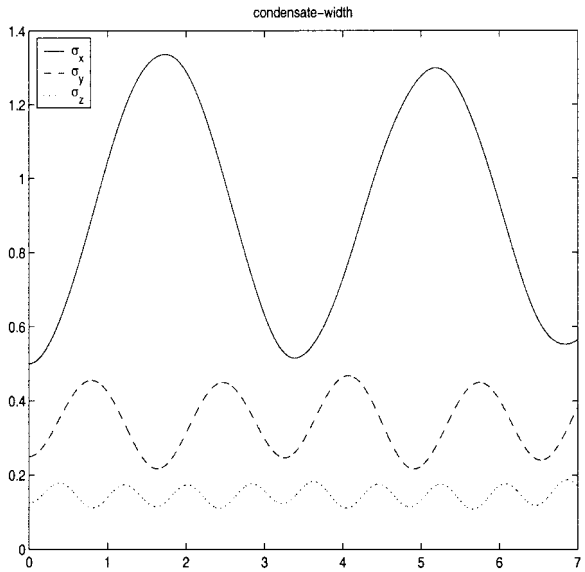

FIG. 4. The time evolutionary plot for the 3D anisotropic condensate width of the case $\gamma_y = 2$, $\gamma_z = 4$.

V. CONCLUSIONS

In this article, we have developed a simple Dufort-Frankel type scheme for solving the time-dependent Gross-Pitaevskii equation in different symmetric geometries. The GPE is a nonlinear Schrödinger equation describing the Bose-Einstein condensation at very low temperature. We present the detailed time and spatial discretization for the equation in three different geometries including the 1D spherically symmetric, 2D cylindrically symmetric, and 3D anisotropic Cartesian domains. The present finite difference scheme has three major advantages: it is explicit, linearly unconditional stable, and is able to handle the coordinate singularities naturally. Furthermore, the scheme is time reversible and satisfies a discrete analogue of density conservation law. The numerical evidence of different test problems shows the validness of our scheme. It is our belief that the present numerical scheme can be applied to further complex time-dependent BEC problems.

APPENDIX
Discrete Density Conservation of the Dufort-Frankel Scheme

As shown in the Introduction, the GPE (1.7) preserves the L_2 norm of the wave function as (1.10). It is desirable for a finite difference scheme to preserve this quantity at the discrete level. In [12, 13], the authors have investigated some discrete conservation of the Dufort-Frankel scheme for 1D linear and nonlinear Schrödinger equations in Cartesian coordinates. In this appendix, we shall derive a discrete analogue of density conservation for the 1D spherically symmetric GPE (3.1):

$$i\frac{\partial \psi}{\partial t} = -\frac{1}{2r^2}\frac{\partial}{\partial r}\left(r^2\frac{\partial \psi}{\partial r}\right) + \frac{1}{2}r^2\psi + \kappa|\psi|^2\psi. \tag{A1}$$

Here, we rewrite the Laplacian term as a divergence form. Note that, the following derivation can be extended to the 2D cylindrically symmetric and 3D cases without any difficulty.

To proceed, we introduce some notations first. As before, we truncate the infinite domain to a large computational domain $[0, R]$ such that the solution is set to be $\psi(R, t) = 0$. We then choose a spatial mesh $\Delta r = R/M$ and define the spatial grid points

$$r_{j-1/2} = (j - 1)\Delta r, \qquad r_j = (j - 1/2)\Delta r, \qquad r_{j+1/2} = j\Delta r, \qquad 1 \le j \le M. \tag{A2}$$

The numerical approximation ψ_j is defined at the grid point r_j so that the boundary value $\psi_{M+1} = 0$. We also define the discrete l_2 norm of ψ_j by

$$\|\psi\|^2 = \sum_{j=1}^{M} r_j^2 |\psi_j|^2 \Delta r. \tag{A3}$$

One should notice that the above numerical integration is simply the midpoint rule for the integral in (3.2).

Now we discretize the equation (A1) by the Dufort-Frankel type scheme:

$$i\,\frac{\psi_j^{n+1} - \psi_j^{n-1}}{2\Delta t} = -\frac{1}{2r_j^2}\left(r_{j+1/2}^2\,\frac{\psi_{j+1}^n - \widetilde{\psi_j^n}}{\Delta r} - r_{j-1/2}^2\,\frac{\widetilde{\psi_j^n} - \psi_{j-1}^n}{\Delta r}\right)\Big/\Delta r + \frac{1}{2}\,r_j^2\,\widetilde{\psi_j^n} + \kappa|\,\widetilde{\psi_j^n}|^2\,\widetilde{\psi_j^n}, \tag{A4}$$

where $\widetilde{\psi_j^n} = (\psi_j^{n+1} + \psi_j^{n-1})/2$. Multiplying the equation (A4) by the term $2\,\overline{\widetilde{\psi_j^n}}\,r_j^2\Delta r$ ($\bar{z}$ is the complex conjugate of z), and making the summation over $j = 1$ to M, we obtain

$$i\sum_{j=1}^{M}(\psi_j^{n+1} - \psi_j^{n-1})2\,\overline{\widetilde{\psi_j^n}}\,r_j^2\Delta r = 2\Delta t\sum_{j=1}^{M} r_j^4|\,\widetilde{\psi_j^n}|^2\Delta r + 4\Delta t\kappa\sum_{j=1}^{M} r_j^2|\,\widetilde{\psi_j^n}|^4\Delta r -$$

$$\frac{\Delta t}{\Delta r^2}\sum_{j=1}^{M}(r_{j+1/2}^2(\psi_{j+1}^n - \widetilde{\psi_j^n}) - r_{j-1/2}^2(\psi_j^n - \psi_{j-1}^n))2\,\overline{\widetilde{\psi_j^n}}\Delta r.$$

Taking the imaginary part of the above equation and using the definition of the discrete l_2 norm, we obtain

$$\|\psi^{n+1}\|^2 - \|\psi^{n-1}\|^2 = -\frac{\Delta t}{\Delta r^2}\,Im\left\{\sum_{j=1}^{M}(r_{j+1/2}^2\psi_{j+1}^n + r_{j-1/2}^2\psi_{j-1}^n)2\,\overline{\widetilde{\psi_j^n}}\Delta r\right\}. \tag{A5}$$

Adding $\|\psi^n\|^2$ to the both sides and substituting the definition of $\widetilde{\psi_j^n}$ into the above equation, we can obtain

$$\|\psi^{n+1}\|^2 + \|\psi^n\|^2 + \frac{\Delta t}{\Delta r^2}\,Im\left\{\sum_{j=1}^{M}(r_{j+1/2}^2\psi_{j+1}^n + r_{j-1/2}^2\psi_{j-1}^n)\overline{\psi_j^{n+1}}\Delta r\right\}$$

$$= \|\psi^n\|^2 + \|\psi^{n-1}\|^2 - \frac{\Delta t}{\Delta r^2}\,Im\left\{\sum_{j=1}^{M}(r_{j+1/2}^2\psi_{j+1}^n + r_{j-1/2}^2\psi_{j-1}^n)\overline{\psi_j^{n-1}}\Delta r\right\}$$

$$= \|\psi^n\|^2 + \|\psi^{n-1}\|^2 + \frac{\Delta t}{\Delta r^2} Im \left\{ \sum_{j=1}^{M} (r_{j+1/2}^2 \overline{\psi_{j+1}^n} + r_{j-1/2}^2 \overline{\psi_{j-1}^n}) \psi_j^{n-1} \Delta r \right\}$$

$$= \|\psi^n\|^2 + \|\psi^{n-1}\|^2 + \frac{\Delta t}{\Delta r^2} Im \left\{ \sum_{j=1}^{M} (r_{j+1/2}^2 \psi_{j+1}^{n-1} + r_{j-1/2}^2 \psi_{j-1}^{n-1}) \overline{\psi_j^n} \Delta r + r_{1/2}^2 (\overline{\psi_0^n} \psi_1^{n-1} - \overline{\psi_1^n} \psi_0^{n-1}) \Delta r \right\}$$

$$= \|\psi^n\|^2 + \|\psi^{n-1}\|^2 + \frac{\Delta t}{\Delta r^2} Im \left\{ \sum_{j=1}^{M} (r_{j+1/2}^2 \psi_{j+1}^{n-1} + r_{j-1/2}^2 \psi_{j-1}^{n-1}) \overline{\psi_j^n} \Delta r \right\}. \qquad [r_{1/2} = 0 \text{ in (A2)}]$$

Therefore, we derive a discrete analogue of density conservation as

$$\|\psi^{n+1}\|^2 + \|\psi^n\|^2 + \frac{\Delta t}{\Delta r^2} Im \left\{ \sum_{j=1}^{M} (r_{j+1/2}^2 \psi_{j+1}^n + r_{j-1/2}^2 \psi_{j-1}^n) \overline{\psi_j^{n+1}} \Delta r \right\} \equiv C. \tag{A6}$$

The authors thank Professor Tsin-Fu Jiang for his helpful discussion and the referees for their suggestions to improve the original version of this article.

References

1. M. H. Anderson, J. R. Ensher, M. R. Matthews, C. E. Wieman, and E. A. Cornell, Observation of Bose-Einstein condensation in a dilute atomic vapor, Science 269 (1995), 198–201.
2. K. B. Davis, M.-O. Mewes, M. R. Andrews, N. J. van Druten, D. S. Durfee, D. M. Kurn, and W. Ketterle, Bose-Einstein condensation in a gas of sodium atoms, Phys Rev Lett 78 (1995), 3969–3973.
3. F. Dalfovo, S. Giorgini, L. P. Pitaevskii, and S. Stringari, Theory of Bose-Einstein condensation in trapped gases, Rev Mod Phys 71(3) (1999), 463–512.
4. S. K. Adhikari, Numerical study of the spherically symmetric Gross-Pitaevskii equation in two space dimensions, Phys Rev E 62(2) (2000), 2937–2944.
5. W. Bao, D. Jaksch, and P. A. Markowich, Numerical solution of the Gross-Pitaevskii equation for Bose-Einstein condensation, J Comput Phys 187 (2003), 318–342.
6. M. M. Cerimele, M. L. Chiofalo, F. Pistella, S. Succi, and M. P. Tosi, Numerical solution of the Gross-Pitaevskii equation using an explicit finite-difference scheme: an application to trapped Bose-Einstein condensates, Phys Rev E 62(1) (2000), 1382–1389.
7. M. M. Cerimele, F. Pistella, and S. Succi, Particle-inspired scheme for the Gross-Pitaevskii equation: an application to Bose-Einstein condensation, Comput Phys Commun 129 (2000), 82–90.
8. Q. Chang, E. Jia, and W. Sun, Difference schemes for solving the generalized nonlinear Schrödinger equation, J Comput Phys 148 (1999), 397–415.
9. E. P. Gross, Structure of a quantized vortex in boson systems, Nuovo Cimento 20 (1961), 454–477.
10. L. P. Pitaevskii, Vortex lines in an imperfect Bose gas, Sov Phys JETP 13 (1961), 451–454.
11. J. C. Strikwerda, Finite difference schemes and partial differential equations, Wadsworth & Brooks/Cole, 1989.
12. L. Wu, Dufort-Frankel-type methods for linear and nonlinear Schrödinger equations, SIAM J Numer Anal 33(4) (1996), 1526–1533.
13. F. Ivanauskas and M. Radžiūnas, On convergence and stability of the explicit difference method for solution of nonlinear Schrödinger equations, SIAM J Numer Anal 36(5) (1999), 1466–1481.

14. P. A. Markowich, P. Pietra, C. Pohl, and H. P. Stimming, A Wigner-measure analysis of the Dufort-Frankel scheme for the Schrödinger equation, SIAM J Numer Anal 40(4) (2002), 1281–1310.

15. P. A. Ruprecht, M. J. Holland, K. Burnett, and M. Edwards, Time-dependent solution of the nonlinear Schrödinger equation for Bose-condensed trapped neutral atoms, Phys Rev A 51 (1995), 4704–4711.

16. W. Bao, S. Jin, and P. A. Markowich, On time-splitting spectral approximation for the Schrödinger equations in the semi-classical regime, J Comput Phys 175 (2002), 487–524.

17. W. Bao, S. Jin, and P. A. Markowich, Numerical study of time-splitting spectral discretizations of nonlinear Schrödinger equations in the semi-classical regimes, SIAM J Sci Comput 25(1) (2003), 27–64.

18. W. Bao and J. Shen, A fourth-order time-splitting Laguerre-Hermite pseudo-spectral method for Bose-Einstein condensates, preprint, 2003.

19. M.-C. Lai and W.-C. Wang, Fast direct solvers for Poisson equation on polar and spherical geometries, Numer Methods Partial Differential Eq 18 (2002), 56–68.

20. W. Bao and Q. Du, Computing the ground state solution of Bose-Einstein condensates by a normalized gradient flow, preprint, 2003.

21. M. J. Holland, D. S. Jin, M. L. Chiofalo, and J. Cooper, Emergence of interaction effects in Bose-Einstein condensation, Phys Rev Lett 78 (1997), 3801–3805.